RSC Advances

ROYAL SOCIETY OF CHEMISTRY

www.rsc.org/advances

RSC Advances

RSCPublishing

PAPER

Investigation on Heat Resistance, Wettability and Hemocompatibility of Polylactide Membrane via Surface Crosslinking Induced Crystallization

Cite this: DOI: 10.1039/x0xx00000x

Received 00th January 2012,
Accepted 00th January 2012

DOI: 10.1039/x0xx00000x

www.rsc.org/

Zhu Xiong, Fu Liu*, Ailin Gao, haibo Lin, Xuemin Yu, Yunze Wang, Yi Wang

Polylactide (PLA) has attracted much attention as a sustainable and environmentally friendly material. However, the poor heat resistance restrains its potential application as porous membrane. Herein, PLA membrane with excellent heat resistance, hydrophilicity and hemocompatibility was developed via a surface crosslinking induced crystallization strategy, which involved two key reactions, namely, copolymerization of N-vinyl-2pyrrolidone (NVP) and triethoxyvinylsilane (VTES) and the subsequent hydrolysis condensation on the surface of PLA membrane. Attenuated total reflectance Fourier transform infrared spectra (ATR-FTIR), X-ray photoelectron spectroscopy (XPS), differential scanning calorimetry (DSC), and X-ray diffraction (XRD) were applied to analyse the surface chemistry and crystallization evolution, which confirmed that P(VP-VTES) copolymer was hydrothermally crosslinked and induced the crystallization of PLA membrane. The surface crystallization significantly improved the heat resistance and preserved membrane morphology, which was characterized by scanning electron microscope (SEM), atomic force microscopy (AFM), and the dimension shrinkage. The modified PLA membrane with χ_c ~37% kept almost unchanged dimension and morphology even by annealing at 100 ^oC for 5 min. The improved hemocompatibility was verified by the prolonged clotting time and recalcification time, which was consistent with the enhanced hydrophilicity. All results showed that surface crosslinking induced crystallization strategy simultaneously improved the heat resistance and hemocompatibility, indicating a promising method for preparing robust and compatible PLA membranes.

Introduction

Biomedical membranes, which remove biological metabolites, endotoxins, harmful micromolecules, and excess water from blood via diffusive and convective transport, have played an important role as artificial kidney, artificial liver, or artificial lung for some organ insufficiency patients[1]. Polysulfone (PS) and polyether sulfone (PES) are extensively investigated and applied as dialysis membranes due to their excellent chemical inertness, mechanical strength, and thermal stability[2-4]. However, the future of petroleum-based PS or PES membrane is confined due to the inevitable one-time consumption of biomedical membranes, which consequently produce massive non-degradable medical waste and cause serious environmental pollution, for example, more than 50 million dialysis modules per year are consumed and disposed in the mainland of China. Moreover, the long-term dialysis through the hydrophobic PS or PES with insufficient biocompatibility will cause dialysis complication and blood coagulation.

Thereof, the bio-based polylactide (PLA), as the sustainable and biodegradable thermoplastic polyester[5-8], is a promising biomedical membrane that possesses less environmental stress and better biocompatibility. Thus far, PLA porous membrane have been widely prepared for drug loading[9], tissue engineering scaffolds[10], water purification[11-14] and hemodialysis[15-17] via the non-solvent induced phase separation. However, PLA membranes are not strong enough for sterilization under high temperature or irradiation probably due to the amorphous structure and low heat-deformation temperature around 60 ^oC. Therefore, it is impossible to achieve the practical application of PLA membranes without conquering the fatal thermo-instability of PLA[8]. Moreover, high porosity and thin thickness will cause more serious deterioration of PLA membranes under heating. The trial studies on PLA porous materials are mostly focusing on the structure regulation and compatible modification. Almost no attention is being paid onto the heat resistance of PLA membranes.

Recently, many researchers have reported the modification of PLA with good thermo-stability in the field of injection, foaming and film blowing et al[5-7]. They all concluded that crystallization played a key role for improving the thermostability. A higher crystallization will increase the heat deflection temperature (HDT) and Vicat penetration temperature more than 30 and 100 ^oC

respectively[8]. However, the overall nucleation and crystallization rates of PLA in homogeneous conditions are relatively low. Although, tremendous efforts have been made to improve PLA crystallization kinetics by blending nucleants to increase its nucleation density and by adding plasticizers to increase chain mobility[8], the conventional melting-blended nucleating agents or plasticizers are not suitable for PLA membrane. Such additives may dissolve out and flow away from the membrane as pore-forming agents during the phase inversion[13]. Although a wide variety of effective nucleating agents like N,N-ethylenebis(12-hydroxystearamide) (EBH) [18], ethylene bis-stearamide (EBS)[19] and 1,3,5-benzene tricarboxyamide (BTA)[20] or plasticizes like triethyl citrate (TEC) [21], Poly(ethylene glycol) (PEG)[22] and fatty acid ester[23] have been used for PLA composite, most of which are toxic and harmful for human and environment due to the bio-toxicity.

However, it is well known that PLA is relatively hydrophobic in nature[6], which results in low cell affinity and elicits an inflammatory response from the living host upon direct contact with biological fluids[24, 25]. Moreover, the crystallization could increase the hydrophobicity and decrease the biocompatibility of PLA. A study by Drieskens et al[26] showed that oxygen and water vapor permeability coefficients of crystallized PLA were decreased by more than 4 and 3 times respectively, compared to amorphous references. Obviously, how to fabricate a PLA membrane with desirable hydrophilicity, anticoagulation and fouling resistance is a key issue for biomedical applications[27, 28].

In recent years, the design of integrated biocompatibility has attracted great attention for implantable and blood contacting membranes, especially for the hydrophobic PS or PES. Higuchi et al [29] prepared a hydrophilic PS membrane covalently conjugated by polyvinylpyrrolidone (PVP) on the surface, and found that PVP-g-PS membrane gave lower protein adsorption from a plasma solution. Meanwhile, the PVP-g-PS membrane showed a much suppressed number of adhering platelets on the surface than neat PS. It is concluded that the hydrophilic surface of the PVP layer on the surface of PS membrane without ionic groups causes the suppression of platelet adhesion on the PVP-g-PS membrane. The similar results were also obtained by Ran et al and Nie et al[30, 31]. The persistent incorporation of PVP or its copolymers rather than simple blending will effectively improve the hydrophilcity and biocompatibility of PLA membranes[32-34]. Therefore, it is of much interest to improve the crystallization and biocompatibility of PLA membranes simultaneously by developing an efficient, feasible and environmental friendly method. Breaking through the bottleneck of poor heat resistance is necessary to achieve the practical application of PLA membranes in biomedical and filtration areas.

In the present work, we aim to develop a surface crosslinking strategy to modify PLA membrane. PLA membrane was simply immersed into a prepolymer P(VP-VTES) for certain time and then treated by a hydrothermal process. The crystallization was induced by the surface crosslinking to enhance the thermo-resistance of PLA membrane substantially. Meanwhile, the hydrophilicity was also improved by the persistent immobilization of P(VP-VTES) on the membrane surface. Specifically, FTIR, DSC and XRD were implemented to study the surface induced crystallization. The influence of surface crystallization on membrane morphology and heat resistance was thoroughly evaluated. Besides, the hydrophilicity, permeability and hemo-compatibility were characterized in aspects of contact angle, water flux, clotting time and recalcification time respectively.

Experimental section

2.1 Materials and regents

Polylactide (PLA) (2003D, Mn=110K-120K Dalton, Natural Works, US) dried at 80 ºC for 24 h was used to prepare membrane. The 1-methyl-2-pyrrolidinone (NMP, AR, Aladdin, China) was used as the solvent to dissolve PLA. NVP (1-vinyl-2-pyrrolidone), VTES (Vinyltrimethylsilane), TEP (Triethyl phosphate) and 2,2'-Azobis(2-methylpropionitrile) (AIBN) all purchased from the Aladdin chemical reagent Co. were directly used to prepare prepolymer P(VP-VTES). The anticoagulant sheep whole blood was purchased from Beijing Pingrui Biotechnology Company, China to characterize the hemocompatibility of PLA membrane.

2.2 Preparation of PLA membrane

PLA porous membranes were prepared via non-solvent induced phase inversion as follows: firstly, 18 g PLA were fully dissolved in 82 g NMP at 80 ^{o}C to form the homogenous solution, and then bubbles were removed by vacuum deaeration at 80 ^{o}C for 5 min. After that, the formed homogenous solution was immediately casted onto a clean glass plate via a blade with a gap of 200 μm, and then solidified in water bath at room temperature for 15 min. After the total solidification, the membranes were soaked into deionized water for 24 h to remove the residue. Lastly, the obtained PLA membranes with the area 150 mm×200 mm were dried at room temperature for 48 h for further modification and characterization.

2.3 Surface crosslinking of PLA membrane

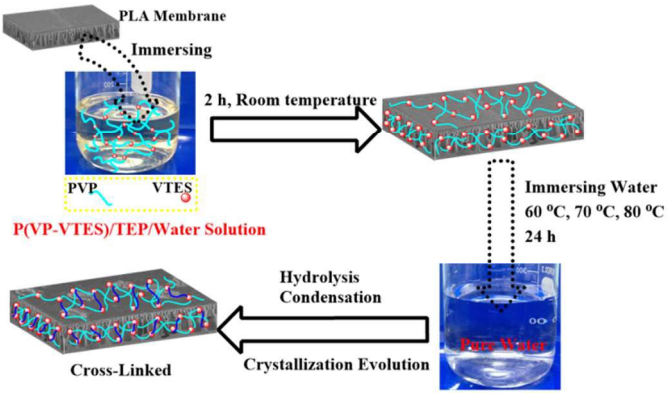

Fig.1. Schematic illustration for the preparation of PLA membranes via P(VP-VTES) surface crosslinking

Prepolymer P(VP-VTES) was first synthesized via free radial polymerization as follows: 6.5 g monomers composed of NVP and VTES with molar ratio of 7/3 were added into the 100 g TEP followed by the addition of 0.08 g AIBN dissolved in 2.5 g TEP. The polymerization was carried out at 80 ^{o}C with vigorous stirring under a nitrogen atmosphere for 18 h to obtain the P(VP-VTES)/TEP solution. Subsequently, the dried PLA membrane (~1g)

with the dimension of 10 cm × 20 cm × 110 μm were fully immersed into the P(VP-VTES)/TEP/water ternary solution (100w/6.5w/100w) for 2 h. After that, the pretreated PLA membranes were transferred in fresh water bath at 60, 70, 80 °C for 24 h for a hydrothermal treatment to boost surface cross-linking and also induce surface crystallization, as shown in Figure1. The so modified PLA membranes were accordingly marked as sample d, e, and f respectively. The modified PLA membranes were rinsed five times by fresh water to remove the uncrosslinked components. As a contrast, the neat PLA membranes without any treatment, the PLA membranes treated by pure water at 60 °C for 24 h, the PLA membranes treated by water/TEP (50/50 w/w) for 24 h were respectively labelled as sample a, b, c. Lastly, all membranes were dried at room temperature for 48 h for further characterization.

2.4 Characterization of PLA membranes

Attenuated total reflectance Fourier transform infrared spectra (ATR-FTIR, Thermo-Nicolet 6700, US) were used to detect functional groups on PLA membrane surface. The surface chemistry of PLA membrane was analyzed using X-ray photoelectron spectroscopy (XPS, Shimadzu Axis Utltradld, Japan) with Mg Kα excitation radiation. The crystallized evolution of the PLA membranes after modification was characterized by differential scanning calorimetry (DSC) on a METTLER TOLEDO TGA/DSC1 analyzer. Firstly, the samples were kept at 30 °C for 3 min before they were heated to 200 °C at 10 ◦C/min, and then degree of crystallinity (χ_c) were determined according to Eq. (1) [35, 36]

$$\chi_c(\%) = \frac{\left(\Delta H_m - \Delta H_c\right) \times 100}{93.6 \times \delta_{PLA}} \quad (1)$$

where ΔH_m and ΔH_c are the enthalpies (J/g) of fusion at melt temperature and crystallization of the PLA membranes, respectively; 93.6 J/g is the enthalpy of fusion of a PLA crystal of infinite size; and δ_{PLA} is the PLA content in PLA membranes. All samples were tested in triplicate.

The X-ray diffraction (XRD) system was used to examine crystal type of PLA membranes. XRD patterns were performed on a D8 Advance diffractometer (Bruker AX, Germany) with a Cu Kα radiation (λ_α=0.154 nm). The equipment was operated at 40 kV and 40 mA under ambient temperature. Samples were scanned in fixed time mode with 7 min under diffraction angle 2 θ in the range of 5-40°.

Membrane morphologies were observed by field emitting scanning electronic microscopy (SEM, Hitachi S-4800, Japan). All samples were sputtered with gold for 2 min for observation. An atomic force microscopy (AFM, Dimension 3100V, Veeco, US) was carried out to determine the surface roughness.

The thermo-resistance of PLA porous membrane was characterized by measuring the area shrinkage after putting the sample (70 cm ×50 cm) in an oven at 100 ºC for 5 min. The shrinkage area was calculated as Eq.2:

$$S = \left(1 - \frac{A_0}{A_r}\right) \times 100\% \quad (2)$$

where A_0 and A_r were the area before and after thermo-treatment.

The hydrophilicity of PLA membrane was characterized by water contact angle measurements (CA, OCA20, Data physics, Germany). A piece of 1×5 cm^2 membrane sample was attached onto a glass slide and 1.0 μL distilled water was dropped onto the air-side surface of the membrane at room temperature. The water contact angle decaying with drop age was recorded by speed optimum video measurement technique.

The pure water flux was measured by using a filtration apparatus (Saifei Company, China). The membranes were pre-pressured at 0.2 MPa about 30 min by deionized water, then the flux was recorded every 10 min at 0.1 MPa until stable. The average value of pure water flux from three tests based on the Eq.3 was obtained for each sample.

$$J = \frac{V}{S \times t} \quad (3)$$

where J (L/m^2·h) is the flux, V (L) is the volume of the permeated pure water, S (4.9 cm^2) is the effective filtration area, t (h) is the operation time.

To evaluate the antithrombogenicity of modified PLA membranes, activated partial thromboplastin time (APTT) was measured by an automated blood coagulation analyzer CA-50 (Sysmex Corporation, Kobe, Japan) as follows: at the beginning of the APTT test, anticoagulant sheep whole blood was collected using vacuum tubes, containing sodium citrate as an anticoagulant (anticoagulant to blood ratio, 1: 9 v/v), and the platelet-poor plasma (PPP) was obtained after centrifuging at 2000 rpm for 15 min and 4000 rpm for 15 min, respectively. Synchronously, All PLA samples (1.0 cm × 1.0 cm, three pieces) washed with PBS (pH 7.4) buffer solution three times were put into the 24-well plate. And then, 0.1 mL of fresh PPP was introduced into each sample using pipette. After maintained at 37 °C for 10 min, 50 μL incubated PPP was added into a test cup, followed by adding 50 μL APTT agent (incubated 10 min before use), and incubated at 37 °C for 5 min. Thereafter, 50 μL $CaCl_2$ (0.025 M) solution was added. Lastly, APTT was obtained by averaging three recordings.

100 μL platelet-poor plasma (PPP, 37 °C) was transferred to a sample surface in a 48-well cell culture plate and incubated at 37 °C for 1 min. Then, 100 μL $CaCl_2$ (0.025M) aqueous solution was added to the membrane sample and the addition time was accurately recorded. The mixture of PPP and $CaCl_2$ solution held on the membrane surface was stirred gently with a stainless-steel hook until the fibrin threads appeared. The duration was recorded as the plasma recalcification time (PRT). Each PRT value was calculated by averaging six measurements.

3. Results and discussion

3.1 Surface chemistry and crystallization of modified PLA membrane

The surface chemistry of PLA membranes modified by surface crosslinking was analyzed by ATR-FTIR and XPS in Figure 2. Compared to the original PLA membrane a, no significant changes appear in PLA membrane b and c, which was treated by water and

TEP solution in 60 °C. However, modified PLA membrane d, e, f showed new peaks at 912 cm^{-1} and 1294 cm^{-1} ascribed to the crystallization of PLA, which is in accordance with the results from Kaewkan and Pan[37, 38], Moreover, the intensity of the crystallization bands at 912 cm^{-1} and 1294 cm^{-1} increased gradually with increasing the hydrothermal-treatment temperature. It is thought that the hydrophilic copolymer P(VP-VTES) on the membrane surface induced the chain segment rearrangement and subsequent crystallization through the plasticization of TEP. However, the ATR-FTIR spectra of the PLA membranes did not show the fine characteristic peaks of the P(VP-VTES).

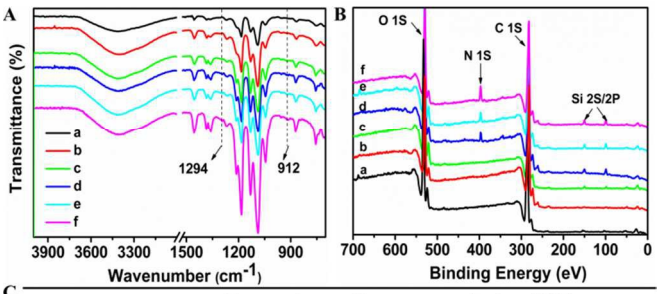

C

Samples	Percentage of components (mol %)				
	C	O	N	Si	P
a	63.1	36.9	/	/	/
b	62.8	37.2	/	/	/
c	62.2	36.8	/	/	/
d	62.4	30.6	3.8	3.2	/
e	63.7	29.6	4.1	3.6	/
f	64.1	27.0	4.8	4.1	/

Fig. 2. ATR-FTIR spectra (A) and XPS wide scans (B) of PLA membranes. The elemental mole percentages of the membranes (C).

In order to reveal the crosslinking reaction of P(VP-VTES) on the PLA membrane surface, XPS was further employed to confirm the fine surface chemistry. The wide scans spectra and the elemental molar percentages are shown in Figure 2B. The PLA membranes simply treated by water and TEP/Water (50/50 w/w) showed same peaks with those of original PLA membrane. However, the peaks of N (1s) and Si (2s/2p) were observed in Figure 2B(d, e, f), indicating the P(VP-VTES) copolymer are present in surface crosslinking PLA membranes via hydrolysis and condensation. Meanwhile, the mass concentration of N (1s) and Si (2s/2p) was increased with increasing the temperature of hydrothermal-treatment, implying that the hydrolysis condensation was accelerated at higher temperature. The *in-situ* crosslinking of VTES and PVP in PVDF casting solution and subsequent phase separation has been already proved in our previous study[32, 33]. It is our first time to accomplish the surface crosslinking of P(VP-VTES) on PLA membrane.

Unexpectedly, the crystallinity and crystal form of PLA membranes was substantially influenced by surface crosslinking. DSC thermograms of PLA membranes with the heating rate of 10°C/min were shown in Figure 3 A. The neat PLA membrane without any treatment shows a glass transition at 63 °C (T_g) and an exothermic cold crystallization peak (T_c) at 100 °C, and the degree of crystallinity χ_c of the neat PLA membrane is zero. No crystallization diffraction peaks are present in Figure 3C(a), showing the neat PLA membrane a is entirely amorphous. Similar thermal properties were observed for PLA membrane b treated with hot water at 60 °C, implying the hot water treatment has almost no effect on the crystallization of PLA membrane. While PLA membrane was treated by TEP/water (50/50 w/w) at 60 °C, both T_g and T_c are decreased due to the plasticizing effect of TEP to some extents. Meanwhile, a value of χ_c about 6% and a small crystallization diffraction peak occurred in membrane c.

Nevertheless, the plasticizing effect of TEP is still confined toward PLA membrane. Interestingly, the crosslinking by only 6.5 w% P(VP-VTES) in TEP/Water solution can promote the crystallization of PLA membranes considerably. As shown in Figure 3A, T_c of modified PLA membrane d was decreased to 93 °C, and χ_c was increased to 13 %. Furthermore, T_g and T_c of modified PLA membrane e, f almost disappeared with increasing the temperature to 70, 80 °C. Accordingly, χ_c of modified PLA membrane e, f is remarkably increased up to about 27%, 37 % respectively as shown in Figure 3B. Meanwhile, the crystallization diffraction peaks at 15°, 17°, 19° and 22° attributed to the PLA' α crystal form[39, 40] occurred in Figure 3C for modified PLA membrane e, f. From the results above, it is inferred that the surface crosslinking of P(VP-VTES) was achieved on PLA membrane surface and consequently induced the crystallization evolution. And higher hydrothermal treatment temperature promoted the surface crystallization significantly.

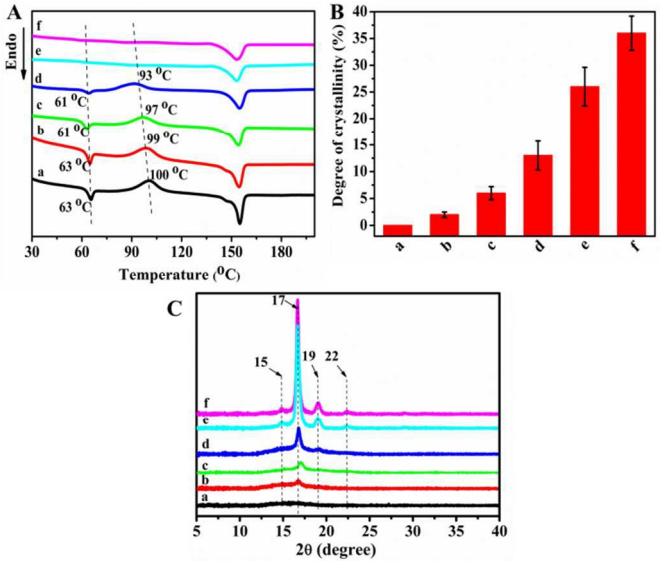

Fig. 3. DSC thermograms (A), degree of crystallinity (B) and wide-angle X-ray diffraction (WAXD) (C) of PLA membranes.

3.2 Morphology of modified PLA membranes

The micro-structure morphologies of modified PLA membranes by surface crosslinking were characterized by SEM in Figure 4. The neat PLA membrane a shows a typical asymmetric structure with finger-like pores and dense top surfaces[41]. The finger-like pores and the smooth surface were completely damaged and contracted due to the thermo-instability of PLA as expected[8], when PLA membrane b was immersed in hot water at 60 °C for 12 h. Interestingly, the modified PLA membrane c treated by TEP/water solution remains

almost unchanged. The crystallization with 6% χ_c induced by TEP plasticization plays an important role on impeding the heat-deformation of PLA membrane in 60 ^oC water. Furthermore, PLA membrane d modified by surface crosslinking preserves the entire microporous structure of PLA membrane with 13% χ_c. With increasing the hydrothermal-treatment temperature to 70 and 80 ^oC, the finger-like pores in the cross section of modified PLA membrane e_1 and f_1 are both perfectly preserved from deterioration due to their higher χ_c. However, more irregular micropores occurred on the top surface as shown in Figure 4e, f, caused by the surface induced crystallization and crystal growth. As reported by Saeidlou[8], the overall crystallization process is typically including two independent phenomena: initial crystal nucleation and subsequent crystal growth. Similarly, the crystallization process of PLA membrane c and d could be dominated by the initial crystal nucleation, and thus their χ_c were both low and showed a smooth top surface. While the surface crosslinking temperature was increased, the subsequent crystal growth was prevailing in PLA membrane e and f, which enhanced χ_c and caused the obvious surface crystallization and irregularly distributed crystal polymorphism and pores on the top surface. Thus, it was demonstrated that the common thermo-instability and the easy heat deformation of PLA membrane was successfully conquered by the feasible surface crosslinking induced crystallization strategy.

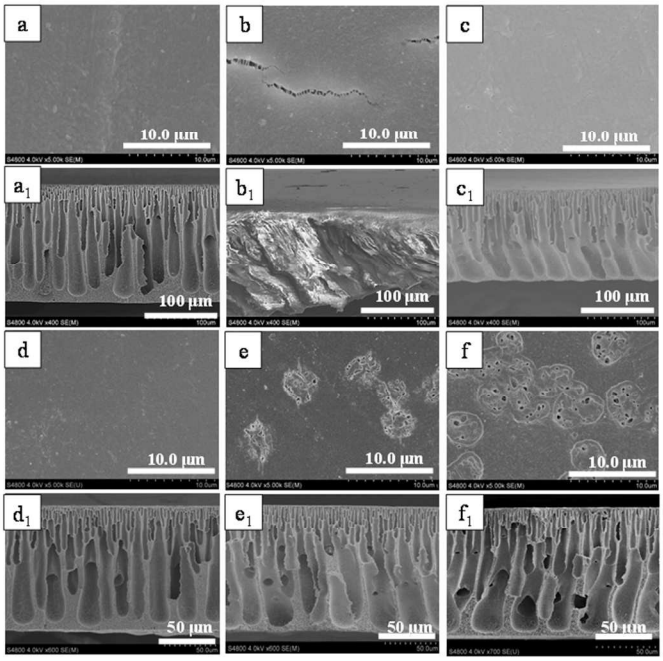

Fig. 4 Surface SEM images (a~f) and the cross-session SEM images (a_1~f_1) of PLA membranes with and without P(VP-VTES) modification.

3.3 Wettability of Modified PLA Membranes

The hydrophilicity of modified PLA membrane was measured by contact angle as shown in Figure 5A. We can see that the contact angle of modified PLA membrane d, e, f was significantly decreased in contrast to that of PLA membrane a, b, c. For example, the initial contact angle of neat PLA membrane a is approximately 84^o and decreased to 75 ^{o} in 300s, and the PLA membrane b and c keeps similar contact variation with time, indicating the relative hydrophobicity. Besides, the membrane a, b, c was still white and not wetted by water in 5 min.

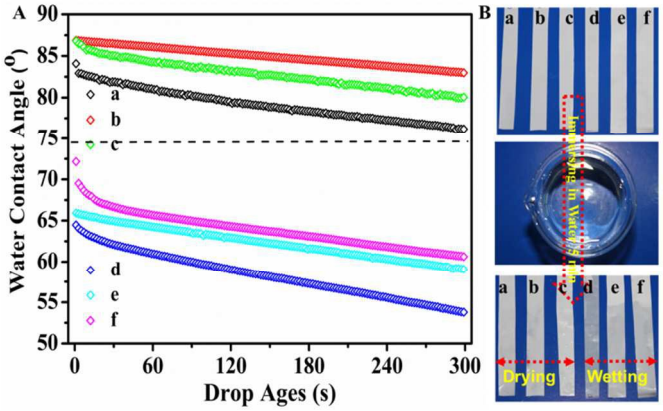

Fig. 5. The typical curves of water contact angle decaying with drop age for PLA membranes (A) and their wettability (B)

However, the modified PLA membrane d exhibited decreased contact angle from 65^o to 53^o, and also it turns transparent and totally wetted by water in 5 min. The enhanced wettability was mainly caused by the surface immobilization of highly hydrophilic PVP segments[32, 33]. The contact angle of modified PLA membrane e, f was increased and both membranes were partially wetted comparing with membrane d. The increased roughness and crystallinity was thought to enhance the hydrophobicity[42-44]. The roughness of membrane e and f was increased to 6.17 nm and 10.00 nm from 4.15 nm as shown in Figure 6, which was consistent with the SEM observation in Figure 4e, f. Therefore, the surface crosslinking of P(VP-VTES) effectively improved the hydrophilicity, whereas the excessive crosslinking caused a more coarse and crystalline surface and subsequently depressed the hydrophilicity slightly.

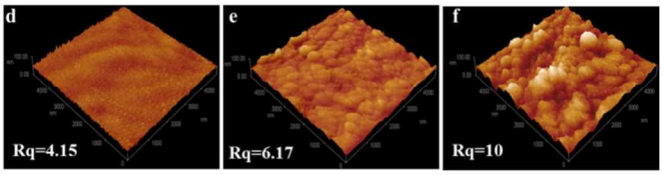

Fig.6. Surface AFM images of the hydrophilic modified PLA membranes (d, e, f).

3.4 Hemocompatibility of Modified PLA Membranes

PLA has been used as tissue engineering materials for a long time. So its histocompatibility including cell adhesion, anti-inflammatory, cytotoxicity etc has been researched in depth[45]. However, blood compatibility of PLA membrane has not been verified reliably[15, 16]. The blood compatibility of modified PLA membrane was investigated in terms of the clotting time and recalcification time as well as the pure water flux, as shown in Figure 7. Generally, the modified PLA membranes d, e, f exhibited longer clotting time and recalcification time in contrast to the unmodified membrane a, b, c. For example, the clotting time and recalcification time of modified

PLA membrane d was extended to ~33 s and ~263 s from ~21 s and ~200 s of neat PLA membrane a, implying that hemocomptibility was substantially improved by the surface crosslinking of hydrophilic P(VP-VTES). Besides, the pure water flux of the modified PLA membrane d was increased to 43 L/ m^2·h due to the enhanced hydrophilicity. The crosslinking P(VP-VTES) was able to bind water molecules and form a hydration layer on the membrane surface, which acts as an energy barrier to prevent the adsorption of blood platelets on PLA membrane surface[29-31]. The similar results were also well reported by Telford via the thermal cross-linking of PNVP on Polystyrene (PS) films[46].

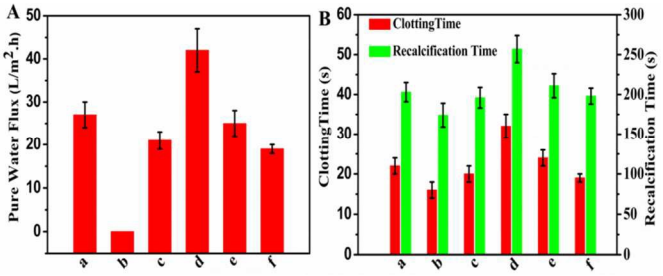

Fig.7. Pure water flux (A), clotting time (B) and Plasma recalcification time (B) of PLA membranes

For modified PLA membrane e and f with higher hydrothermal temperature, the clotting time and recalcification time were shortened to some extends, accordingly both membranes exhibited declined water flux due to the higher crystallinity, roughness and decreasing wettability. The coagulation factor VII of the blood is easily activated when the blood is contacting with the rough surface, and the thrombin will be produced from thrombinogen via the stepped active process[15, 47]. PLA membrane b showed the lowest clotting time and recalcification time as well as the lowest pure water flux due to the serious membrane curling and contraction under 60 ^{o} water treatment. The influence of crystallization on the permeability of PLA membranes was also in accordance with the previous report. For example Drieskens et al reported that the vapour permeability of PLA was decreased by more than 3 times with increasing the crystallization[26].

3.5 Thermo-Stability of Modified PLA Membranes

One general drawback of PLA is the lower heat deflection temperature (HDT) (~60 ^{o}C). The thermal dimension and microporous structure stability was especially crucial to the membrane performances. Actually, there is an urgent requirement for the membrane drying and disinfection at high temperature. While the amorphous neat PLA membrane was treated at 100 ^{o}C for 5 min, it was shrinking and curling tremendously as shown in Figure 8A(a). The shrink rate was ~42% as shown in Figure 8B(a). Meanwhile, the micro-structure in terms of top surface and cross section also appeared serious deterioration in Figure 8C(a, a_1), implying that the filtration function was completely lost. However, the modified PLA membrane d with ~13% χ_c demonstrated a shrink rate ~26% at 100^{o}C for 5 min. And also the microstructure was still affected severely as shown in Figure 8C(d, d_1). With enhancing the hydrothermal temperature, the modified PLA membranes (e, f) with the sufficient χ_c exhibited a quite stable dimension and porous structure under heating. Especially for membrane f with ~37% χ_c, its dimension and pore structure remained almost unchanged as well as the microstructure. As proved previously,[8, 48, 49] if the χ_c in PLA reached over 30%, its heat deflection temperature (HDT) would be increased to over 100 ^{o}C. Thereafter, the enhanced crystallization induced by the surface crosslinking effectively improved the thermostabiliy of PLA porous membrane with the thin thickness of about 200 μm. The modified PLA membrane f with ~37 % χ_c can successfully withstand the strict annealing at 100 ^{o}C for 5 min.

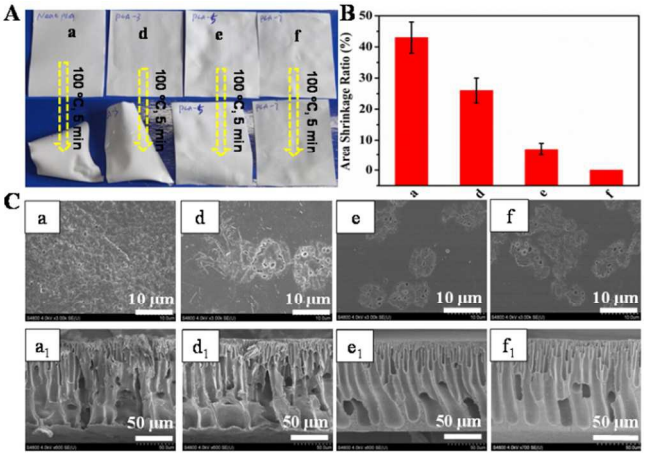

Fig.8. The heat deformation (A), heat shrinkage rate (B), surface SEM images [C(a, d, e, f)] and the cross-session SEM images (a_1, d_1, e_1, f_1) of the neat PLA (a) and modified PLA membranes (d, e, f) under 100 ^{o}C for 5 min

As mentioned above, it was well known that the crystallization induced by surface self-crosslinking played a key role on the thermo-stability of PLA membranes. In this section, the flux and blood compatibility of annealing PLA membranes were discussed in details. As shown in Figure 9A(a), the water flux of the amorphous neat PLA membrane after annealing was declined to 0, and the clotting time and recalcification time are decreased due to the coarse surface. Similar results are also observed in membrane d. The lower crystallinity cannot resist the surface and micro-porous structure deterioration under high temperature annealing, despite its hydrophilic modification with P(VP-VTES). While the crystallinity of PLA membrane e and f is high to 27 %, and 37 %, the corresponding pure water flux, clotting time and recalcification time remained almost unchanged after annealing, indicating the good stability of membrane performance. For example, the membrane e still showed a water flux of ~21 L/m^2.h, clotting time of ~23 s and recalcification time ~223 s of after heat treatment. Therefore, it was demonstrated that the surface crosslinking promoted the crystallization of PLA membranes, and consequently improved the thermostability in aspects of dimension, microstructure, permeability and hemocompatibility.

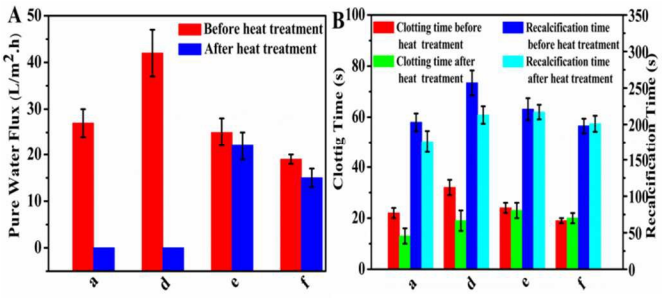

Fig.9. The pure water flux (A), clotting time (B), and Plasma recalcification time (B) of the neat PLA (a) and modified PLA membranes (d, e, f) before and after heat treatment under 100 °C for 5 min

Conclusion

A feasible approach for producing heat resistant and hemocompatible PLA membranes by surface crosslinking was developed in this work. Hydrophilic P(VP-VTES) was persistently anchored on PLA membranes to enhance the hydrophilicity, water permeability and hemocompatibility. More interestingly, the surface crystallization evolution was achieved and promoted with increasing hydrothermal treatment temperature. Both surface chemistry and morphologies confirmed the surface crosslinking and crystallization evolution clearly. However, the hydrophilicity, permeability and hemocompatibility of the modified PLA membranes were slightly depressed with excessive crosslinking. The specific PLA membrane with χ_c ~37% exhibited excellent thermostability in aspects of dimension, microstructure, permeability and hemocompatibility under a strict thermal treatment at 100 °C for 5 min. Therefore, the present work provided a feasible surface crosslinking strategy to solve the bottleneck of thermo-instability of PLA membrane. Besides, the hydrophilicity and hemocompatibility were significantly improved, indicating its great potential application as a robust and hemocompatible membrane.

Acknowledgements

This work is supported by National Natural Science Foundation of China (51473177, 51273211), China's Postdoctoral Science Funding (2015M581965), and Natural Science Foundation of Ningbo (2015A610024).

Notes and references

Ningbo Institute of Materials Technology & Engineering, Chinese Academy of Sciences, Ningbo, 315201, P. R. China
Tel.: 86-574-86685256; E-mail: fu.liu@nimte.ac.cn

Electronic Supplementary Information (ESI) available: [details of any supplementary information available should be included here]. See DOI: 10.1039/b000000x/

1. C. Cheng, S. Sun, and C. Zhao, *J. Mater. Chem. B*, 2014, **2**, 7649-7672.
2. A. Nabe, E. Staude and G. Belfort, *J. Membr. Sci*, 1997, 133, 57-72.
3. J. K. Park, M. H. Acar, A. Akthakul, W. Kuhlman and A. M. Mayes, *Biomaterials*, 2006, **27**, 856-865.
4. B. Fang, Q. Ling, W. Zhao, Y. Ma, P. Bai, Q. Wei and C. Zhao, *J. Membr. Sci*, 2009, **329**, 46-55.
5. J. M. Raquez, Y. Habibi, M. Murariu and P. Dubois, *Prog. Polym. Sci*, 2013, **38**, 1504-1542.
6. R. M. Rasal, A. V. Janorkar, and D. E. Hirt, *Prog. Polym. Sci*, 2010, **35**, 338-356.
7. M. Nofar and C. B. Park, *Prog. Polym. Sci,* 2014, **39**, 1721-1741.
8. S. Saeidlou, M. A. Huneault, H. Li, and C. B. Park, *Prog. Polym. Sci*, 2012, **37**, 1657-1677.
9. S. A. Hagan, A. G. A. Coombes, M. C. Garnett, S. E. Dunn, M. C. Davies, L. Illum and P. R. Gellert, *Langmuir*, 1996, **12**, 2153-2161.
10. D. W. Hutmacher, *Biomaterials*, 2000, **21**, 2529-2543.
11. T. Tanaka and D. R. Lloyd, *J. Membr. Sci,* 2004, **238**, 65-73.
12. P. Shen, A. Moriya, S. Rajabzadeh, T. Maruyama and H. Matsuyama, *Desalination*, 2013, **325**, 37-39.
13. A. Moriya, T. Maruyama, Y. Ohmukai, T. Sotani and H. Matsuyama, *J. Membr. Sci,* 2009, **342**, 307-312.
14. A. Moriya, P. Shen, Y. Ohmukai, T. Maruyama, H. Matsuyama, *J. Membr. Sci,* 2012, **415**, 712-717.
15. A. L. Gao, F. Liu, L. X. Xue, *J. Membr. Sci*, 2014, **452**, 390-399.
16. L. J. Zhu, F. Liu, X. M. Yu, A. L. Gao, and L. X. Xue, *J. Membr. Sci,* 2015, **475**, 469-479.
17. X. M. Yu, F. Liu, L. Z. Wang, Z. Xiong, and Y. Z.Wang, *RSC. Adv*, 2015, **5**, 78306-78314.
18. J. Y. Nam, M. Okamoto, H. Okamoto, M. Nakano, A. Usuki, and M. Matsuda, *Polymer*, 2006, **47**, 1340-1347.
19. A. M. Harris, and E. C. Lee, *J. Appl. Polym. Sci,* 2008, **107**, 2246-2255.
20. H. Nakajima, M. Takahashi, and Y. Kimura, *Macromol.Mater. Eng*, 2010, **295**, 460-468.
21. L. V. Labrecque, R. A. Kumar, V. Dave, R. A. Gross, and S. P. McCarthy, *J. Appl. Polym. Sci*, 1997, **66**, 1507-1513.
22. M. Sheth, R. A. Kumar, V. Davé, R. A. Gross, S. P. McCarthy, (1997). *J. Appl. Polym. Sci*, 1997, **66**, 1495-1505.
23. I. Pillin, N. Montrelay, and Y. Grohens, *Polymer*, 2006, **47**, 4676-4682.
24. B. D. Ratner, *Biosens. Bioelectron*, 1995, **10**, 797-804.
25. K. J. L. Burg, W. D. Holder, C. R. Culberson, R. J. Beiler, K. G. Greene, A. B. Loebsack and C. R. Halberstadt, *J. Biomat. Sci-Polym. E*, 1999, **10**, 147-161.
26. M. Drieskens, R.. Peeters, J. Mullens, D. Franco, P. J. Lemstra and D. G. Hristova-Bogaerds, *J. Polym. Sci. Pol. Phy,* 2009, **47**, 2247-2258.
27. Q. Yu, Y. Zhang, H. Wang, J. Brash and H. Chen, *Acta. Biomater*, 2011, **7**, 1550-1557.
28. Z. Ma, Z. Mao, and C. Gao, *Colloid. Surface. B*, 2007, **60**, 137-157.
29. A. Higuchi, K. Shirano, M. Harashima, B. O. Yoon, M. Hara, M. Hattori, and K. Imamura, *Biomaterials*, 2002, **23**, 2659-2666.
30. F. Ran, S. Nie, W. Zhao, J. Li, B. Su, S. Sun, and C. Zhao, *Acta. Biomater*, 2011, **7**, 3370-3381.
31. S. Nie, J. Xue, Y. Lu, Y. Liu, D. Wang, S. Sun and C. Zhao, *Colloid. Surface. B*, 2012, **100**, 116-125.
32. M. M. Tao, F. Liu and L. X. Xue, *J. Membr. Sci*, 2015, **474**, 224-232.
33. M. M. Tao, L. X. Xue, F. Liu, and L. Jiang, Adv. Mater, 2014, **26**, 2943-2948.
34. M. Henry and P. Bertrand, *Surf. Interface. Anal*, 2009, **41**, 105-113.
35. Z. Xiong, Y. Yang, J. X. Feng, C. Z. Zhang, Z. B. Zhang, and J. Zhu, *Carbohyd. Polym*, 2013, **92**, 810-816.
36. Z. Xiong, C. Li, S. Q. Ma, J. X. Feng, Y. Yang, C. Z. Zhang and J. Zhu, Carbohyd. Polym, 2013, **95**, 77-84.
37. K. Wasanasuk, and K. Tashiro, *Macromolecules*, 2011, **44**, 9650-9660.
38. P. Pan, J. Yang, G. Shan, Y. Bao, Z. Weng, A. Cao and Y. Inoue, *Macromolecules*, 2011, **45**,189-197.
39. C. F. Yang, Y. F. Huang, J. Ruan, and A. C. Su, *Macromolecules*, 2012, **45**, 872-878.
40. C. Y. Chen, C. F. Yang, U. S. Jeng, and A. C. Su, *Macromolecules*, 2014, **47**, 5144-5151.
41. A. L. Gao, F. Liu, H. Y. Shi and L. X. Xue, *J. Membr. Sci*, 2015, **478**, 96-104.
42. T. G. Ruardy, J. M. Schakenraad, H. C. Van der Mei, and H. J. Busscher *J. Biomed. Mater. Res. A*, 1995, **29**, 1415-1423.
43. T. Groth and G. Altankov, *Biomaterials*, 1996, **17**, 1227-1234.
44. D. Murray, T. Rae, and N. Rushton, *J. Bone. Joint. Surg. Br*, 1989, **71**, 632-637.
45. C. R. Chu, R. D. Coutts, M. Yoshioka, F. L. Harwood, A. Z. Monosov,

and D. Amiel, *J. Biomed. Mater. Res*, 1995, **29**, 1147-1154.
46. A. M. Telford, M. James, L. Meagher, and C. Neto, ACS. *Appl. Mater. Inter*, 2010, **2**, 2399-2408.
47. F. Tong, X. Chen, L. Chen, P. Zhu, J. Luan, C. Mao, and J. Shen, *J. Mater. Chem. B*, 2013, **1**, 447-453.
48. Z. B. Tang, C. Z. Zhang, X. Q. Liu and J. Zhu, *J. Appl. Polym. Sci*, 2012, **125**, 1108-1115.
49. A. M. Harris, and E. C. Lee, *J. Appl. Polym. Sci,* 2008, **107,** 2246-2255.

.

Graphic for manuscript